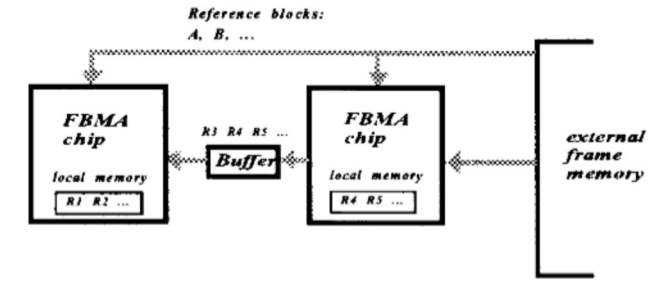

(a)

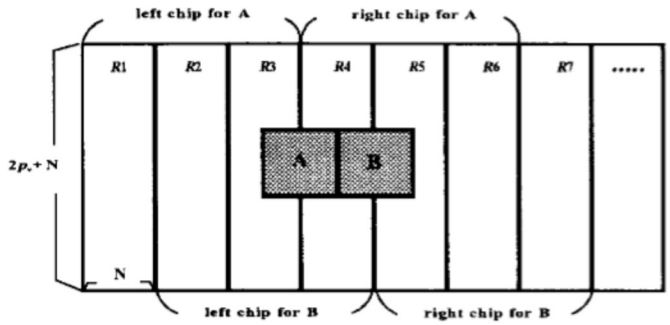

(b)

Fig. 4. Cascading two chips for doubling horizontal search range: (a) block diagram of cascading two chips and (b) search area for two chips.

in a search area using simply two search data input flows, and by the continuous process between blocks. We have implemented the processor for $-16/+15$ search ranges in a total of 220k gates using 0.6 μm triple-metal CMOS technology. It has been shown that the operating clock runs up to 66 MHz. Therefore, its application scope can contain the encoding H.263(4CIF), MPEG2(MP@ML), and other multimedia applications.

REFERENCES

[1] J. R. Jain and A. K. Jain, "Displacement measurement and its application in interframe image coding," *IEEE Trans. Commun.*, vol. COM-29, pp. 1799–1808, Dec. 1981.
[2] L. D. Vos and M. Stegherr, "Parameterizable VLSI architectures for the full search block matching algorithm," *IEEE Trans. Circuits Syst.*, vol. 36, pp. 1309–1316, Oct. 1989.
[3] T. Komarek and P. Pirsch, "Array architectures for block matching algorithms," *IEEE Trans. Circuits Syst.*, vol. 36, pp. 1301–1308, Oct. 1989.
[4] STI3220, *Image Processing Databook*, SGS-Thomson Microelectron., Oct. 1992.
[5] K. Ishihara *et al.*, "A half-pel precision MPEG2 motion estimation processor with concurrent three-vector search," in *ISSCC, Dig. Tech. Papers*, Feb. 1995, pp. 288–289.
[6] K. M. Yang, M. T. Sun, and L. Wu, "A family of VLSI design for the motion compensation block matching algorithm," *IEEE Trans. Circuits Syst.*, vol. 36, pp. 1317–1325, Oct. 1989.
[7] S. H. Nam and M. K. Lee, "Flexible VLSI architecture of motion estimator for video image compression," *IEEE Trans. Circuits Syst. II*, vol. 43, pp. 467–470, June 1996.
[8] C.-H. Hsieh and T. P. Lin, "VLSI architecture for block matching motion estimation algorithm," *IEEE Trans. Circuits Syst. Video Technol.*, vol. 2, pp. 169–175, June 1992.
[9] A. Ohtani *et al.*, "A motion estimation processor for MPEG2 video real time encoding at wide search range," in *Proc. CICC*, 1995, pp. 17.4.1–17.4.4.
[10] K. Suguri *et al.*, "A real-time motion estimation and compensation LSI with wide-search range for MPEG2 video encoding," in *ISSCC, Dig. Tech. Papers*, Feb. 1996, pp. 242–243.
[11] A. Horng-Dar Lin *et al.*, "A 14GOPS programmable motion estimator for H.26X," in *ISSCC, Dig. Tech. Papers*, Feb. 1996, pp. 246–247.
[12] Draft for ITU-T Recommendation H.263, *Video Coding for Low Bitrate Communication*.
[13] ISO/IEC 13818-2, *Generic Coding of Moving Pictures and Associated Audio Information, Part 2: Video*.

Lossy Synthesis of Digital Lattice Filters

Louiza Sellami and Robert W. Newcomb

***Abstract*— A new method for converting a lossless cascade lattice realization of a real, stable, single-input, single-output $(\mathrm{ARMA}n, m)$ filter, with a lossy constant terminating one-port section, to a lossy realization is proposed. The conversion process is carried out through the factorization of the transfer scattering matrix of a two-port equivalent of the terminating section and the distribution of the loss term, embedded in this matrix, among the lossless lattice sections according to some desirable pattern. The cascade is then made computable through the extraction of right-matched J-unitary normalization sections. The technique applies to both degree-one and degree-two lattice sections, and is rendered systematic owing to the particular lossless lattice structure used. The motivation for this work lies in the synthesis of a pipeline of digital cochlea lattices with loss suitable for hearing impairment diagnosis via Kemp echoes.**

***Index Terms*— Computable lossy filters, digital lattice filters, passive synthesis.**

I. INTRODUCTION

In [1], we proposed a new technique to synthesize a real, stable, single-input, single-output ARMA(n, m) filter as a cascade of degree-one or degree-two real lossless lattice sections from the reflection coefficient and the zeros of transmission (real or complex), with a minimum number of delay elements. The technique relies on a four-step complex Richard's function extraction where two steps are used for degree reduction, and the other two for obtaining real degree-two sections from complex degree-one sections. The resulting structure is terminated on a lossy constant real one-port section after all of the dynamics is extracted through repeated lossless extractions. In the present paper, we develop a new technique to obtain a lossy cascade structure from a lossless one with lossy termination while preserving its passivity and realness properties. The key idea is to distribute the loss term, embedded in the terminating section, among the lattice sections in such a fashion as to include a loss term locally, according to some desirable pattern. Since the resulting sections are not computable, i.e., admit delay-free loops, we transform them to

Manuscript received July 16, 1996; revised March 12, 1997. This paper was recommended by Associate Editor B. A. Shenoi.

L. Sellami is with the Department of Electrical Engineering, US Naval Academy, Annapolis, MD 21402 USA (e-mail: sellami@eng.umd.edu) and also with the Department of Electrical Engineering, University of Maryland, College Park, MD 20742 USA.

R. W. Newcomb is with the Department of Electrical Engineering, University of Maryland, College Park, MD 20742 USA (e-mail: newcomb@eng.umd.edu).

Publisher Item Identifier S 1057-7130(98)02151-X.

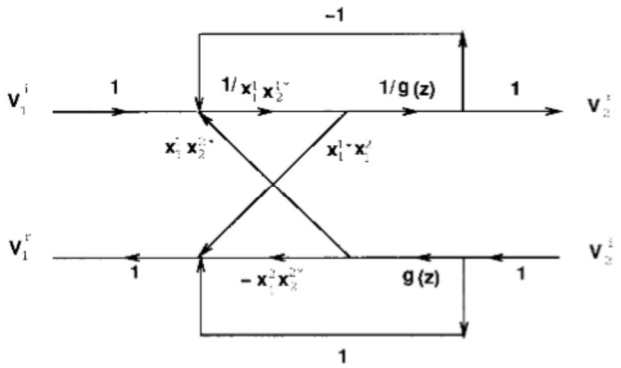

Fig. 1. Signal flow graph of the degree-one section of (1). Here, $g(z) = (z-1)/[(1a^*)(z-a)]$.

computable sections following the ideas of Deprettere and Dewilde [2]. To achieve this, we use the following procedures.

- Conversion of the terminating lossy load from a one-port to a lossy loaded two-port, and construction of its transfer scattering matrix θ_R.
- Factorization of θ_R in the form $\theta_R = \Pi_{i=1}^{n} \theta_{R_i}$.
- Distribution of the θ_{R_i} matrices among the lossless lattice sections.
- Realization of the lossy structure with no delay-free loops.

A typical application of this technique is the implementation of cochlea lattice filters for cochlea characterization from noninvasive measurements of stimulated acoustic emissions (also known as Kemp echoes) [3]. Since the cochlea has some loss embedded in the basilar membrane, it is important to incorporate this loss in the lattice filter model so that an accurate assessment of the characteristic parameters of the ear can be achieved.

II. Preliminaries

In the following sections, we will rely heavily on the concepts of lossless lattice synthesis of ARMA filters developed in [1] for the structure and properties of the lossless lattice realization, and [4] for the concepts of network synthesis. Therefore, here we assemble those main results, as well as present passivity conditions for a lossy section.

Here and in the following, the superscripts $*$ and T denote complex conjugation and matrix transposition, respectively, while the subscript $*$ denotes para-Hermitian conjugation, i.e., $A_*(z) = A^{*T}(1/z^*)$ for a matrix $A(z)$. We define the transfer scattering matrix $\theta_{x_1x_2}(z)$ of a section as the matrix that gives the signals $[V_1^i, V_1^r]^T$ at the left port when multiplied by the signals $[V_2^r, V_2^i]^T$ at the right port. Each degree-one section with nonunit zero of transmission and normalized to $\theta_{x_1x_2}(1) = I_2$ is described by a 2×2 transfer scattering matrix of the form [1], [2]

$$\theta_{x_1x_2}(z) = I_2 + \frac{(z-1)}{(1-a^*)(z-a)} x_1 x_{2*} J \tag{1}$$

where I_2 is the 2×2 identity matrix, a is the zero of transmission being realized with $a \neq 1$, x_1, and x_2 are two constant, possibly complex, vectors, and J is given by

$$J = \begin{bmatrix} 1 & 0 \\ 0 & -1 \end{bmatrix}. \tag{2}$$

The signal flow diagram of (1) is shown in Fig. 1.

If the section is passive, the transfer scattering matrix is J-expansive, i.e., $\theta_{x_1x_2}^{*T}(z) J \theta_{x_1x_2}(z) - J \geq 0$ in $|z| > 1$ where ≥ 0 means positive semidefinite. If the section is lossless, the transfer scattering matrix is J-para-unitary, i.e., $\theta_{x_1x_2}(z)_* J \theta_{x_1x_2}(z) = J$, as well as J-expansive in $|z| > 1$.

For a lossless passive section, x_1 and x_2 are such that $x_1 = x_2 = x = [x^1, x^2]^T$ and $x_* J x = |a^2| - 1$, resulting from the J-para-unitary property, although for a lossy section described by (1), the vectors $x_1 = [x_1^1, x_1^2]^T$ and $x_2 = [x_2^1, x_2^2]^T$ may be chosen equal. But in any event, $\theta_{x_1x_2}(z)$ does not satisfy the J-para-unitary condition. In [1], it was shown that the lossless section of (1) could be realized as a cascade of two lattice sections: a delay lattice cascaded with a constant lattice as shown in Fig. 2. As can be seen from Fig. 2, the section is stable since, for $|a| > 1$, the section has a pole at $1/a^*$ which is inside the unit circle, and for $|a| < 1$, the section has a pole at a which is also inside the unit circle. Moreover, it was proven in [2] that such a lattice filter can always be realized with no delay-free loops.

A degree-two real lossless lattice section is realized as a cascade of two degree-one lossless lattice sections (of the type shown in Fig. 2) extracting a pair of conjugate zeros of transmission, according to the synthesis technique developed in [1]. The transfer scattering matrix of such a degree-two lattice section is, therefore, obtained as follows [1], [2]:

$$\begin{aligned} \theta(z) &= \left[I_2 + \frac{(z-1)}{(1-a^*)(z-a)} x x_* J \right] \\ &\quad \cdot \left[I_2 + \frac{(z-1)}{(1-a)(z-a^*)} y y_* J \right] \\ &= I_2 + \frac{(z-1)}{|K|^2} \left[\frac{u v_*}{(1-a^*)(z-a)} + \frac{u^* v^T}{(1-a)(z-a^*)} \right] J \end{aligned} \tag{3}$$

where

$$\begin{aligned} &u = x,\ v = Ky^*,\ |K|^2 = 1 - |\gamma|^2 (r^2 + 4d^2)^{-1} \\ &\gamma = u^T J u,\ r = |a|^2 - 1,\ d = \frac{a - a^*}{2j} = \mathrm{Im}(a) \end{aligned} \tag{4}$$

and the last form of (3) results in real elements.

III. Transfer Scattering Matrix of the Terminating Section

We assume the existence of a nonzero lossy passive terminating section in the ARMA realization process, and let S_{in} be the normalized input reflection coefficient and R_{in} the associated "input resistance" of the lossy constant terminating section (Fig. 3); then S_{in} is constant and such that $|S_{\mathrm{in}}| < 1$, and is related to R_{in} through the following equation [4]:

$$S_{\mathrm{in}} = \frac{R_{\mathrm{in}} - 1}{R_{\mathrm{in}} + 1} \Longrightarrow R_{\mathrm{in}} = \frac{S_{\mathrm{in}} + 1}{1 - S_{\mathrm{in}}}, \qquad R_{\mathrm{in}} > 0. \tag{5}$$

Considering that R_{in} can be looked upon as coming from a resistor, we split R_{in} into a series of two positive resistances R and R_L, as shown in Fig. 4, and represent the extracted resistance R as a two-port system for which we write

$$v_1 = R i_1 + v_2 = -R i_2 + v_2, \qquad i_1 = -i_2,$$

and

$$R_{\mathrm{in}} = R + R_L. \tag{6}$$

The corresponding transfer scattering matrix θ_R is given by (see the Appendix for details)

$$\begin{aligned} \theta_R &= I_2 + \frac{R}{2} \begin{bmatrix} 1 & -1 \\ 1 & -1 \end{bmatrix} = I_2 + \frac{R}{2} \begin{bmatrix} 1 \\ 1 \end{bmatrix} [1 \quad -1] \\ &= I_2 + \frac{R}{2} U_o V_o^T, \qquad R \geq 0 \end{aligned} \tag{7}$$

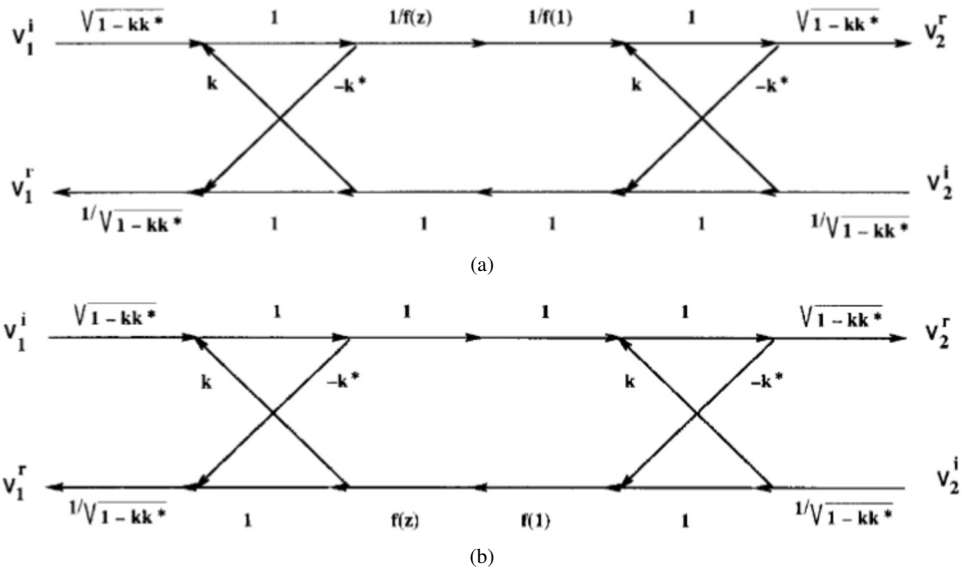

Fig. 2. Signal flow graphs of a degree-one lossless lattice section with $f(z) = (1a^*z)/(z-a)$. (a) $|a| > 1$ and $k = (x^2/x^1)^*$. (b) $|a| < 1$ and $k = (x^1/x^2)^*$.

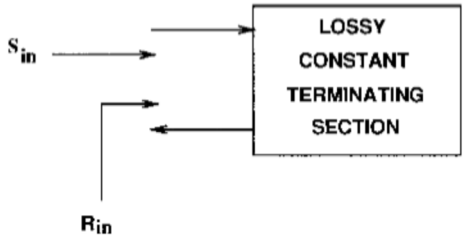

Fig. 3. Lossy constant terminating section.

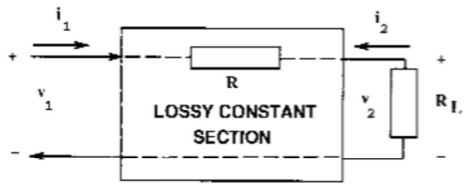

Fig. 4. Extracted resistance R represented as a two-port.

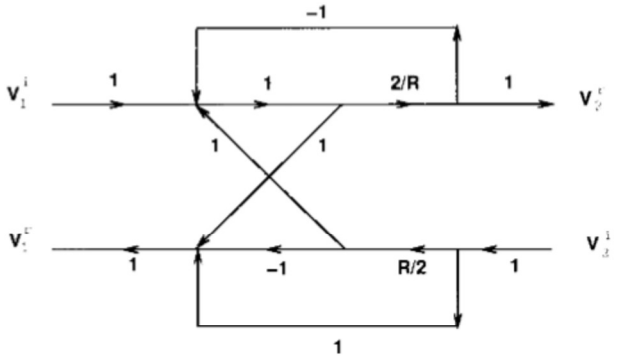

Fig. 5. Signal flow graph of the lossy constant terminating section.

and is in the form of Fig. 1, with the resulting structure shown in Fig. 5 (U_o and V_o being defined for use in Section VI). This structure is naturally suited for describing distributed loss in our cochlea model [5], which drew our attention to the need for lossy sections. Note that, although delay-free loops are highly apparent in the signal flow graph of Fig. 5, we will prove in Section VI that, with the chosen structure for the terminating constant section, the cascaded lossy structure can be made computable through the insertion of right-matched normalization sections.

IV. Transfer Scattering Matrix Factorization

Proposition 1: The transfer scattering matrix θ_R of (7) can be factored as follows:

$$\theta_R = \prod_{i=1}^{n} \theta_{R_i}, \quad \theta_{R_i} = I_2 + \frac{R_i}{2}\begin{bmatrix} 1 & -1 \\ 1 & -1 \end{bmatrix} \tag{8}$$

where the R_i's form any nonnegative partition of R such that

$$R = \sum_{i=1}^{n} R_i \quad \text{and} \quad R_i \geq 0. \tag{9}$$

Proof: Consider two matrices θ_{R_1} and θ_{R_2} as defined in (7); then we have, as $V_o^T U_o = 0$,

$$\theta_{R_1}\theta_{R_2} = I_2 + \frac{R_1 + R_2}{2}\begin{bmatrix} 1 & -1 \\ 1 & -1 \end{bmatrix}. \tag{10}$$

By repeating this process n times, we establish (8). The factorization of θ_R can be represented schematically by a cascade of constant lossy sections of the type shown in Fig. 5 with similar structures, but of differing parameters.

V. Lossy Synthesis Technique

The key to the lossy synthesis technique is the factorization of the transfer scattering matrix of the lossy terminating section (derived in Proposition 1) and the use of the particular structure of the lossless lattice sections proposed in [1]. This structure allows for a systematic conversion from lossless to lossy, as shown in Propositions 2 and 3 below.

Proposition 2—Case of Degree-One Lattice Sections: Any degree-one passive lossless lattice section, of transfer scattering matrix $\theta_{xx}(z)$, cascaded on the right (or left) with a constant lossy section, of transfer scattering matrix θ_R, is equivalent to a degree-one lossy section of transfer scattering matrix $\theta_{y_1y_2}(z)$ cascaded on the left (or right) with the same constant lossy section, as illustrated in Fig. 6,

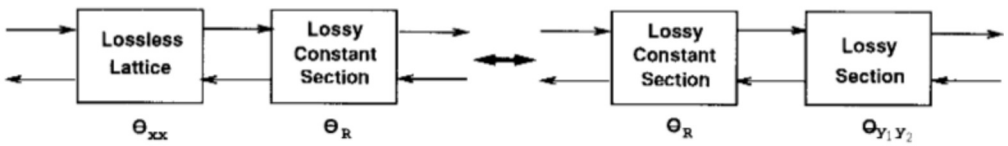

Fig. 6. Transformation of a lossless lattice section to a lossy section.

with

$$y_1 y_{2*} = \theta_R^{-1} x x_* \theta_R^T, \quad y_1 = \theta_R^{-1} x, \quad \text{and} \quad y_2 = \theta_R x. \tag{11}$$

Proof: Assuming the structure of Fig. 6 with identical θ_R on the left and the right gives

$$\left[I_2 + \frac{(z-1)xx_*J}{(1-a^*)(z-a)}\right]\theta_R = \theta_R\left[I_2 + \frac{(z-1)y_1y_{2*}J}{(1-a^*)(z-a)}\right]. \tag{12}$$

The left-hand side of (12) is equal to the right-hand side if and only if

$$\theta_R y_1 y_{2*} J = x x_* J \theta_R, \quad \Longrightarrow y_1 y_{2*} = \theta_R^{-1} x x_* J \theta_R J^{-1}. \tag{13}$$

The solution in (13) always exists since θ_R is nonsingular and its inverse is

$$\theta_R^{-1} = I_2 + \frac{R}{2}\begin{bmatrix}-1 & 1\\ -1 & 1\end{bmatrix} = I_2 - \frac{R}{2}\begin{bmatrix}1 & -1\\ 1 & -1\end{bmatrix}. \tag{14}$$

Since $J^{-1} = J$, we have

$$J\theta_R J^{-1} = I_2 + \frac{R}{2}\begin{bmatrix}1 & 1\\ -1 & -1\end{bmatrix} = \theta_R^T \tag{15}$$

which, when substituted in (13), yields the possible solution

$$y_1 y_{2*} = \theta_R^{-1} x x_* \theta_R^T, \quad y_1 = \theta_R^{-1} x, \quad \text{and} \quad y_2 = \theta_R x = \theta_R^2 y_1 \neq y_1. \tag{16}$$

And because $y_1 \neq y_2$, $\theta_{y_1y_2}(z)$ is lossy. Note that since the left side of (12) is passive, so is the right side, although $\theta_{y_1y_2}(z)$ need not be passive. However, the passivity of $\theta_{y_1y_2}(z)$ is not a concern here since, in the end, we are interested in implementing sections of the type $\theta_R\theta_{y_1y_2}(z)$ which are passive, and thus, at each extraction, the magnitude of the reflection coefficient is less than one in $|z| > 1$.

Proposition 3—Case of Degree-Two Lattice Sections: Any degree-two passive real lossless lattice section, of transfer scattering matrix $\theta_{uv}(z)$, cascaded on the right (or left) with a constant lossy section, of transfer scattering matrix θ_R, is equivalent to a degree-two lossy real section of transfer scattering matrix $\theta_{wx}(z)$ cascaded on the left (or right) with the same constant lossy section with

$$w x_* = \theta_R^{-1} u v_* \theta_R^T, \quad w = \theta_R^{-1} u, \quad \text{and} \quad x = \theta_R v. \tag{17}$$

Proof: We start with

$$\left\{I_2 + \frac{(z-1)}{|K|^2}\left[\frac{uv_*}{(1-a^*)(z-a)} + \frac{u^*v^T}{(1-a)(z-a^*)}\right]J\right\}\theta_R = \theta_R\left\{I_2 + \frac{(z-1)}{|K|^2}\left[\frac{wx_*}{(1-a^*)(z-a)} + \frac{w^*x^T}{(1-a)(z-a^*)}\right]J\right\} \tag{18}$$

and repeat the proof given in Proposition 2. Here, again, by virtue of (12), the cascaded structure remains passive, irrespective of the passivity of $\theta_{wx}(z)$.

Proposition 4: Given the overall transfer scattering matrix $\theta(z)$ of a lattice filter, realized as a cascade of n degree-one or degree-two lossless lattices sections terminated on a constant real lossy section, such that

$$\theta(z) = \theta_1(z)\theta_2(z)\cdots\theta_n(z)\theta_R(z) \tag{19}$$

where $\theta_i(z)$ is the transfer scattering matrix of the ith lossless lattice section as defined in (1), for a degree-one lattice, or (3), for a degree-two lattice, and θ_R is the transfer scattering matrix of the lossy constant terminating section, factored in the form

$$\theta_R = \theta_{R_1}\theta_{R_2}\cdots\theta_{R_n}\theta_{R_L}. \tag{20}$$

Then $\theta(z)$ can be realized as a cascade of n degree-one or degree-two lossy sections terminated on a lossy constant section of transfer scattering matrix θ_{R_L} such that

$$\theta(z) = \tilde{\theta}_1(z)\tilde{\theta}_2(z)\cdots\tilde{\theta}_{n-1}\tilde{\theta}_n\theta_{R_L} \tag{21}$$

where

$$\tilde{\theta}_1(z) = \theta_1(z)\theta_{R_1} \text{ and } \tilde{\theta}_i(z) = \left[\prod_{j=1}^{i-1}\theta_{R_j}\right]^{-1}\theta_i(z)\prod_{j=1}^{i}\theta_{R_j}, \quad \text{for } i = 2, 3, \cdots, n \tag{22}$$

and $\tilde{\theta}_i(z)$ is the transfer scattering matrix describing the ith lossy passive section. If $\theta_i(z)$ is real, then $\tilde{\theta}_i(z)$ is also real.

Proof: For the proof, we use the results of the previous proposition, that is,

$$\theta_{R_i}\hat{\theta}_i(z) = \theta_i(z)\theta_{R_i}, \quad \text{for} \quad i = 1, 2, \cdots, n. \tag{23}$$

This process is repeated n times for $\theta_n(z)$ and yields $\hat{\theta}^{(n)}(z)$, $n-1$ times for $\theta_{n-1}(z)$ and yields $\hat{\theta}^{(n-1)}(z)$, and once for $\theta_1(z)$ and yields $\hat{\theta}^{(1)}(z)$ as shown below:

$$\begin{aligned}
\theta(z) &= \theta_1(z)\theta_2(z)\cdots\theta_{n-1}(z)\theta_n(z)\theta_{R_1}\theta_{R_2}\cdots\theta_{R_{n-1}}\theta_{R_n}\theta_{R_L}\\
&= \theta_1(z)\theta_2(z)\cdots\theta_{n-1}(z)\theta_{R_1}\hat{\theta}_n^{(1)}(z)\theta_{R_2}\cdots\theta_{R_{n-1}}\theta_{R_n}\theta_{R_L}\\
&= \theta_1(z)\theta_2(z)\cdots\theta_{R_1}\hat{\theta}_{n-1}^{(1)}(z)\theta_{R_2}\hat{\theta}_n^{(2)}(z)\theta_{R_3}\cdots\theta_{R_{n-1}}\theta_{R_n}\theta_{R_L}\\
&= \quad\vdots\\
&= \theta_{R_1}\hat{\theta}_1^{(1)}(z)\theta_{R_2}\hat{\theta}_2^{(2)}(z)\cdots\theta_{R_{n-1}}\hat{\theta}_{n-1}^{(n-1)}(z)\theta_{R_n}\hat{\theta}_n^{(n)}(z)\theta_{R_L}\\
&= \tilde{\theta}_1(z)\tilde{\theta}_2(z)\cdots\tilde{\theta}_{n-1}(z)\tilde{\theta}_n(z)\theta_{R_L}
\end{aligned} \tag{24}$$

where

$$\tilde{\theta}_i(z) = \theta_{R_i}\theta_i^{(i)}(z), \qquad \text{for} \quad i = 1, 2, \cdots, n. \tag{25}$$

By the argument given in (12), $\tilde{\theta}_i(z)$ is passive and lossy. With (23)–(25), we establish the algorithm given in (22) for computing the transfer scattering matrices of the lossy sections.

VI. Computable Lossy Sections

For many purposes, it is important that the structure have no delay-free loops, i.e., be computable, for example, when using an iterative calculation where an iteration could not otherwise proceed due to a signal's new value depending on that value itself. Consequently, we follow the technique introduced in [2, pp. 252–253] for lossless

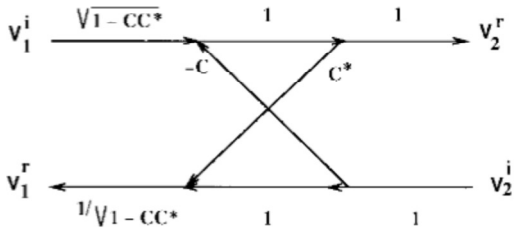

Fig. 7. Signal flow graph of the constant lossless passive section of (26).

structures, and prove here that it is always possible to find an equivalent lossy cascade which has no delay-free loops. To this end, we first perform a transformation on the overall transfer scattering matrix $\theta(z)$ by multiplying it on the right by a constant J-unitary matrix θ_c (for computability). We then factor and distribute θ_c among the sections in such a fashion as to provide for their local normalization, leading to a computable cascade. We proceed from the fact that any constant passive lossless section can be described by a J-unitary transfer scattering matrix of the form

$$\theta_c = \begin{bmatrix} 1 & C \\ C^* & 1 \end{bmatrix} \begin{bmatrix} \theta_c^1 & 0 \\ 0 & \theta_c^2 \end{bmatrix} \tag{26}$$

where $1 - CC^* > 0$ to guarantee that θ_c is J-expansive and θ_c^1 and θ_c^2 must satisfy (27) for θ_c to be J-unitary:

$$|\theta_c^1| = |\theta_c^2| = \frac{1}{\sqrt{1 - CC^*}}. \tag{27}$$

The corresponding signal flow diagram is shown in Fig. 7.

Proposition 5: The transfer scattering matrix θ_c given in (26) can be factored as the product of n J-unitary, J-expansive transfer scattering matrices as follows:

$$\theta_c = \prod_{i=1}^{n} \theta_{ci}, \quad \text{with} \quad \theta_{ci} = \begin{bmatrix} 1 & C_i \\ C_i^* & 1 \end{bmatrix} \begin{bmatrix} \theta_{ci}^1 & 0 \\ 0 & \theta_{ci}^2 \end{bmatrix}. \tag{28}$$

Proof: We give the proof for the case of two matrices; the same procedure can then be repeated to establish the general case. Consider θ_{c1} and θ_{c2} of the form given in (28). Then

$$\begin{aligned} \theta_{c1}\theta_{c2} &= \begin{bmatrix} \theta_{c1}^1\theta_{c2}^1 + C_1C_2^*\theta_{c1}^2\theta_{c2}^1 & C_2\theta_{c1}^1\theta_{c2}^2 + C_1\theta_{c1}^2\theta_{c2}^2 \\ C_1^*\theta_{c1}^1\theta_{c2}^1 + C_2^*\theta_{c1}^2\theta_{c2}^1 & C_1^*C_2\theta_{c1}^1\theta_{c2}^2 + \theta_{c1}^2\theta_{c2}^2 \end{bmatrix} \\ &= \begin{bmatrix} 1 & C \\ C^* & 1 \end{bmatrix} \begin{bmatrix} \theta_c^1 & 0 \\ 0 & \theta_c^2 \end{bmatrix}. \end{aligned} \tag{29}$$

If we choose $\theta_{c1}^1 = \theta_{c1}^{2*}$ and $\theta_{c2}^1 = \theta_{c2}^{2*}$, then the factorization is possible and

$$\theta_c^1 = \theta_c^{2*} = \theta_{c1}^1\theta_{c2}^1 + C_1C_2^*\theta_{c1}^2\theta_{c2}^1 \tag{30}$$

$$C = \frac{C_1\theta_{c1}^2\theta_{c2}^2 + C_2\theta_{c1}^1\theta_{c2}^2}{\theta_c^2}. \tag{31}$$

Proposition 6: Consider θ_{R_i} of the form given in (7) and θ_{ci} of the form given in (28), then the following is always true:

$$\theta_{R_i}\theta_{ci} = \theta_{ci}\hat{\theta}_{R_i} \tag{32}$$

where $\hat{\theta}_{R_i}$ is J-expansive and is given by

$$\hat{\theta}_{R_i} = \theta_{ci}^{-1}\left[I_2 + \frac{R_i}{2}U_oV_o^T\right]\theta_{ci}. \tag{33}$$

Proof: The proof follows directly from Proposition 2. Since θ_{R_i}, θ_{ci}, and θ_{ci}^{-1} are J-expansive, it follows that $\hat{\theta}_{R_i}$ is also J-expansive. Note that $\hat{\theta}_{R_i}$ has the same structure as θ_{R_i}, except that the vectors U_o and V_o^T are replaced by $\theta_{ci}^{-1}U_o$ and $V_o^T\theta_{ci}$, respectively [see (7)].

As a consequence of Propositions 4–6, the J-unitary matrix θ_c can now be distributed among the load sections. In turn, the sections resulting from this process can be distributed among the original lossless sections, thus creating a cascade of sections of the form $\tilde{\theta}_i(z)\tilde{\theta}_{R_i}\theta_{ci}$ as shown below.

$$\begin{aligned} \theta(z) &= [\theta_1(z)\theta_2(z)\cdots\theta_n(z)][\theta_{R_1}\theta_{R_2}\cdots\theta_{R_n}][\theta_{c1}\theta_{c2}\cdots\theta_{cn}] \\ &= [\theta_1(z)\theta_2(z)\cdots\theta_n(z)][\hat{\theta}_{R_1}\theta_{c1}][\hat{\theta}_{R_2}\theta_{c2}]\cdots[\hat{\theta}_{R_n}\theta_{cn}] \\ &= [\tilde{\theta}_1(z)\tilde{\theta}_{R_1}\theta_{c1}][\tilde{\theta}_2(z)\tilde{\theta}_{R_2}\theta_{c2}]\cdots[\tilde{\theta}_n(z)\tilde{\theta}_{R_n}\theta_{cn}]. \end{aligned} \tag{34}$$

Proposition 7: The section described by the transfer scattering matrix $\tilde{\theta}_i(z)\tilde{\theta}_{R_i}\theta_{ci}$ is always computable and is real if $\theta_i(z)$ is real.

Proof: For computability, it is necessary and sufficient to choose C_i so that the (1, 2) entry of $\tilde{\theta}_i(z)\tilde{\theta}_{R_i}\theta_{ci}$ is zero at infinity for $a \neq \infty$. Since $\tilde{\theta}_i(z)$ has the same structure as its lossless counterpart, we have

$$\begin{aligned} \tilde{\theta}_i(z)\tilde{\theta}_{R_i}\theta_{ci} = &\left[I_2 + \frac{(z-1)}{(1-a^*)(z-a)}x_1x_{2*}J\right] \\ &\cdot \theta_{ci}^{-1}\left[I_2 + \frac{R_i}{2}U_oV_o^T\right]\theta_{ci}\frac{1}{\sqrt{1-C_iC_i^*}}\begin{bmatrix} 1 & C_i \\ C_i^* & 1 \end{bmatrix}. \end{aligned} \tag{35}$$

After some calculations, it is seen that the (1, 2) entry is forced to zero by the choice

$$C_i = \frac{(1-a^*)\frac{R_i}{2} + x_1^1x_2^{1*}\frac{R_i}{2} + x_1^1x_2^{2*}\left(\frac{R_i}{2} - 1\right)}{(1-a^*)\left(1+\frac{R_i}{2}\right) + x_1^1x_2^{1*}\left(1+\frac{R_i}{2}\right) + x_1^1x_2^{2*}\frac{R_i}{2}} \tag{36}$$

where C_i satisfies $1 - C_iC_i^* > 0$ imposed by the passivity condition. The factors of (34) are those which will be used recursively to synthesize the computable cascade. The flow graph of each section is obtained by cascading the flow graphs given in Figs. 2, 5, and 7. Note that in the end, we obtain a lossy passive cascade where each section is composed of a lossless passive dynamic section, a lossy passive constant load section, and a lossless passive constant section. It follows that each section is lossy and passive, and thus the magnitude of the load on each section has a reflection coefficient less than or equal to one in $|z| > 1$.

VII. Lossy Synthesis of an ARMA(6, 6) Filter

Here, we illustrate the technique with a simple example in which a lossy-terminated lossless lattice structure implementing a stable ARMA(6, 6) filter is converted to a cascade of lossy structures. The lossless lattice structure is a cascade of three degree-two real lattice filter sections terminated on a constant one-port section. The lossless lattice sections are described by their transfer scattering matrices (taken from [1]) as follows.

For the first lossless lattice filter section, see (37). For the second lossless lattice filter section, see (38). For the third lattice lossless filter section, see (39). The lossy terminating one-port section is characterized by its input reflection coefficient $S_{\text{in}} = 0.39$ and an input resistance $R_{\text{in}} = 2.28$. For simplicity, we choose $R_L = 0$, and divide the input resistance into three equal resistances $R_1 = R_2 = R_3 = R_{\text{in}}/3 = 0.76$. Each lossy constant section is then described by the following transfer scattering matrix:

$$\theta_R = I_2 + \tfrac{0.76}{2}\begin{bmatrix} 1 & -1 \\ 1 & -1 \end{bmatrix}. \tag{40}$$

Next, we compute the transfer scattering matrices of the lossy sections according to the algorithm given in (22) as shown in (41)–(43) at the bottom of the page.

To show that we do get rid of delay free loops, as an example, we apply the technique developed in Section VI to the first section. Since the technique was developed to work with degree-one sections, we factor $\theta_1(z)$ into two degree-one factors, the first of these being characterized by the transfer scattering matrix in (44) at the bottom of the page. We use (36) to calculate the coefficient C, and then form the right-matched normalization factor:

$$\theta_c = \begin{bmatrix} 1.41 & 0.86 - 0.49j \\ 0.86 + 0.49j & 1.41 \end{bmatrix}. \tag{45}$$

The resulting section is shown in (46) at the bottom of the page, which is computable since the (1, 2) term is zero at infinity.

VIII. Discussion

In this paper, we modified the nature of the lattice realization developed in [1] from a cascade of lossless lattice sections to lossy ones by distributing the loss term among the lossless lattices. This is accomplished by converting a portion of the lossy terminating section into a two-port, deriving an associated transfer scattering matrix from its input reflection coefficient, factoring it into a cascade of constant lossy two-ports of the same structure, translating these two-ports from the end of the lossless cascade to the appropriate location, and finally, calculating the new lossy sections. As proven in Propositions 2 and 3, by passing θ_R from the right side of $\theta_{xx}(z)$ to its left side, the proposed technique modifies the nature of each section from lossless to lossy while preserving the structure of Fig. 1. In addition, the technique preserves the realness property of $\theta_{y_1y_2}$ and the passivity property of $\theta_R\theta_{y_1y_2}$ in (12), although $\theta_{y_1y_2}$ may not be passive. However, since in the end we are interested in the implementation of sections of the type given in (12), the passivity of $\theta_{y_1y_2}$ is not a concern here, and thus, is not further investigated at this point. But the computability of the cascade is a major concern for various purposes and, therefore, was discussed and solved. It was shown that the lossy structure could be realized as a computable cascade of lossy sections, each consisting of a lossy dynamic section connected on the right to a constant lossless section. Note that making a real degree-one section computable does not alter the realness. However, the realness for the degree-two case needs further investigation.

The technique applies to both degree-one and degree-two lossless lattices, and is best suited for the lossless synthesis described in [1]. However, with minor modifications, it can be adapted to suit other types of ARMA synthesis such as the ones presented in [6] (two-ports), [7] (four-ports), or [2] (orthogonal multiport digital filters). As with the passive network synthesis techniques, on which the method is based, generalizations to multiports is possible, while of perhaps equal importance would be the insertion of nondynamic nonlinearities between sections.

In the factorization of the transfer scattering matrix of the lossy terminating section, the choice of the parameter R_i in (8) for each factor is not imposed and, therefore, could be adapted to the kind of application being considered. For instance, in the lattice realization of the cochlea models developed in [3], [5], the distribution of the loss term could be chosen to match the damping distribution of the basilar membrane along the cochlea since it is the damping that contributes to the lossy character of the latter. In the more general (nonbiological) ear-type analog and digital systems amenable to a pipeline ear-like structure [8], the resistance R_i would mimic an equivalent parameter characteristic of the system at hand.

Appendix

The admittance matrix Y associated with the two-port of Fig. 4 is given by

$$Y = \frac{1}{R}\begin{bmatrix} 1 & -1 \\ -1 & 1 \end{bmatrix}. \tag{47}$$

The corresponding scattering matrix S_R is determined from the admittance matrix using the relation $S_R = (I_2 + Y)^{-1}(I_2 - Y)$,

$$\tilde{\theta}_1(z) = \theta_1(z)\theta_R = \begin{bmatrix} \dfrac{7.46 - 17.71z + 11.63z^2}{2 - 2z + z^2} & \dfrac{2.32 - 2.53z - 0.18z^2}{2 - 2z + z^2} \\ \dfrac{8.53 - 17.91z + 9.76z^2}{2 - 2z + z^2} & \dfrac{2.93 - 2.33z + 0.02z^2}{2 - 2z + z^2} \end{bmatrix} \tag{41}$$

$$\tilde{\theta}_2(z) = \theta_R^{-1}\theta_2(z)\theta_R^2 = \begin{bmatrix} \dfrac{19.83 - 48.04z + 33.73z^2}{10 - 8z + 2z^2} & \dfrac{0.69 + 9.96z - 12.17z^2}{10 - 8z + 2z^2} \\ \dfrac{23.04 - 47.54z + 26.03z^2}{10 - 8z + 2z^2} & \dfrac{1.81 + 9.46z - 8.79z^2}{10 - 8z + 2z^2} \end{bmatrix} \tag{42}$$

$$\tilde{\theta}_3(z) = \theta_R^{-2}\theta_3(z)\theta_R^3 = \begin{bmatrix} \dfrac{64.94 - 125.09z + 171.93z^2}{90 - 18z + 9z^2} & \dfrac{20.43 + 50.52z - 101.73z^2}{90 - 18z + 9z^2} \\ \dfrac{77.63 - 135.85z + 89.00z^2}{90 - 18z + 9z^2} & \dfrac{36.89 + 61.28z - 47.95z^2}{90 - 18z + 9z^2} \end{bmatrix} \tag{43}$$

$$\begin{aligned} \tilde{\theta}(z) &= I_2 + \frac{z - 1}{z - (1 + j)^*}\begin{bmatrix} 1.73 \\ 1.34 + 0.45j \end{bmatrix}\begin{bmatrix} 1.73 & 1.34 + 0.45j \end{bmatrix}^{T^*} J \\ &= \begin{bmatrix} \dfrac{-1.99 - j + (2.99 + j)z}{1 - j + jz} & \dfrac{(-2.32 + 0.78j)(-1 + z)}{1 - j + jz} \\ \dfrac{(2.32 + 0.78j)(-1 + z)}{1 - j + jz} & \dfrac{2.99 - j + (-1.99 + j)z}{1 - j + jz} \end{bmatrix} \end{aligned} \tag{44}$$

$$\tilde{\theta}(z)\tilde{\theta}_R\theta_c = \begin{bmatrix} \dfrac{-0.69 - 1.37j + (2.31 + 1.19j)z}{1 - j + jz} & \dfrac{0.65 - 0.67j}{1 - j + jz} \\ \dfrac{-0.38 - 0.99j + (1.45 + 1.29j)z}{1 - j + jz} & \dfrac{1.36 - 0.7j + (-0.16 + 0.51j)z}{1 - j + jz} \end{bmatrix} \tag{46}$$

and is given by

$$S_R = \frac{1}{2+R}\begin{bmatrix} R & 2 \\ 2 & R \end{bmatrix} \tag{48}$$

from which we establish (7) by using

$$\theta_R = \begin{bmatrix} S_{R_{21}}^{-1} & -S_{R_{21}}^{-1} S_{R_{22}} \\ S_{R_{11}} S_{R_{21}}^{-1} & S_{R_{12}} - S_{R_{11}} S_{R_{21}}^{-1} S_{R_{22}} \end{bmatrix}. \tag{49}$$

ACKNOWLEDGMENT

The authors wish to thank the reviewers for their constructive comments, especially on the matter of computability.

REFERENCES

[1] L. Sellami and R. W. Newcomb, "Synthesis of ARMA filters by real lossless digital lattices," *IEEE Trans. Circuits Syst. II,* vol. 43, pp. 379–386, May 1996.
[2] E. Deprettere and P. Dewilde, "Orthogonal cascade realization of real multiport digital filters," *Circuit Theory Appl.,* vol. 8, pp. 245–272, July 1980.
[3] L. Sellami, R. W. Newcomb, V. Rodellar, and P. Gomez, "A digital model for cochlea characterization," in *Proc. 5th Int. Conf. Biomed. Eng.*, Spain, Sept. 1994, pp. 15–16.
[4] R. W. Newcomb, *Linear Multiport Synthesis.* New York: McGraw-Hill, 1966.
[5] L. Sellami and R. W. Newcomb, "A digital scattering model of the cochlea," *IEEE Trans. Circuits Syst. I,* vol. 44, pp. 174–180, Feb. 1997.
[6] R. W. Newcomb, N. El-Leithy, V. Rodellar, P. Gomez, and M. Cordoba, "Computable minimum lattice-like ARMA synthesis," *IEEE Trans. Circuits Syst.,* vol. 35, pp. 577–583, May 1988.
[7] T. Cheng, "Realization of transmission lattice filters," Doctoral dissertation, Dep. Elect. Eng., Univ. Maryland, College Park, 1990.
[8] L. Sellami and R. W. Newcomb, "Ear-type analog and digital systems," *Recent Research Developments in Circuits and Systems,* vol. I, pp. 59–83, 1996.

Clock-Controlled Neuron-MOS Logic Gates

Koji Kotani, Tadashi Shibata, Makoto Imai, and Tadahiro Ohmi

***Abstract*—A new clock-controlled circuit scheme has been introduced in the basic architecture of neuron-MOS (neuMOS or νMOS) logic gates. In this scheme, the charge on a neuMOS floating gate is periodically refreshed by a clock-controlled switch. A special refreshing scheme in which fluctuations in device parameters are automatically canceled has been employed. As a result, the number of multiple logic levels that can be handled in a neuMOS floating gate has been increased. In addition, the data subtraction operation directly conducted on the floating gate has become possible. All of these circuit techniques have enhanced the functionality of a neuMOS logic gate a great deal. In order to achieve a low power operation, latched-sense-amplifier circuitries are also introduced for logic decision. Test circuits were fabricated in a double-polysilicon CMOS process, and the basic circuit operations are demonstrated.**

***Index Terms*—Auto zero, clock-controlled logic, latched sense amplifier, neuron-MOS.**

I. INTRODUCTION

The functional capability of a logic integrated-circuit chip has been ever increasing thanks to the remarkable progress in the semiconductor technology. Such functionality enhancement, however, has been achieved so far by primarily increasing the number of gates integrated on a chip. In our previous work [1]–[5], we have proposed an alternative approach to enhance the functionality of a chip, not by merely increasing the number of elements, but by increasing the functional capability of an element. For this purpose, we have introduced a high-functionality transistor called the neuron MOSFET (abbreviated as neuMOS or νMOS for short) [1]. Using neuMOS, a multiple-input thresholding element, the dramatic simplification in logic circuit configurations has been demonstrated as compared to conventional CMOS circuitries [2], [3]. In addition, the high degree of parallelism in hardware computation and the high flexibility in circuit architecture, such as the real-time reconfigurability of circuits, have been realized by neuMOS logic gates, which has presented a great potential for high-density integration of "functionality" on a chip [2]–[8].

A neuMOS transistor is a floating-gate MOS transistor in which multiple-input terminals are capacitively coupled to the floating gate. The complementary inverter configuration is usually employed as

Manuscript received July 16, 1996; revised June 19, 1997. This work was supported in part by the Ministry of Education, Science, Sports, and Culture of Japan under the Grant-in-Aid for Scientific Research on Priority Areas, "Ultimate Integration of Intelligence on Silicon Electronic Systems." A part of this work was carried out in the Super Clean Room of Laboratory for Electronic Intelligent Systems, Research Institute of Electrical Communication, Tohoku University. This paper was recommended by Associate Editor J. M. Zurada.

K. Kotani and M. Imai are with the Department of Electronic Engineering, School of Engineering, Tohoku University, Aza-Aoba, Aramaki, Aoba-ku, Sendai 980-8579, Japan and the Laboratory for Electronic Intelligent Systems, Research Institute of Electrical Communication, Tohoku University, Katahira 2-1-1, Aoba-ku, Sendai 980-8577, Japan (e-mail: kotani, imai@sse.ecei.tohoku.ac.jp).

T. Shibata is with the Department of Information and Communication Engineering, University of Tokyo, 7-3-1 Hongo, Bunkyo-ku, Tokyo 113-8656, Japan (e-mail: shibata@ee.t.u-tokyo.ac.jp).

T. Ohmi is with the Department of Electronic Engineering, School of Engineering, Tohoku University, Aza-Aoba, Aramaki, Aoba-ku, Sendai 980-8579, Japan (e-mail: ohmi@sse.ecei.tohoku.ac.jp).

Publisher Item Identifier S 1057-7130(98)02152-1.